Environmental Science & Technology

pubs.acs.org/est

Article

Life-Course Health Risk Assessment of $PM_{2.5}$ Elements in China: Exposure Disparities by Species, Source, Age, Gender, and Location

Kai Cheng, Yunhua Chang,* Xuhui Lee, Dongsheng Ji, Liping Qiao, Zhong Zou, Yusheng Duan, and Ru-Jin Huang

Cite This: *Environ. Sci. Technol.* 2024, 58, 3629−3640

Read Online

ACCESS | Metrics & More | Article Recommendations | Supporting Information

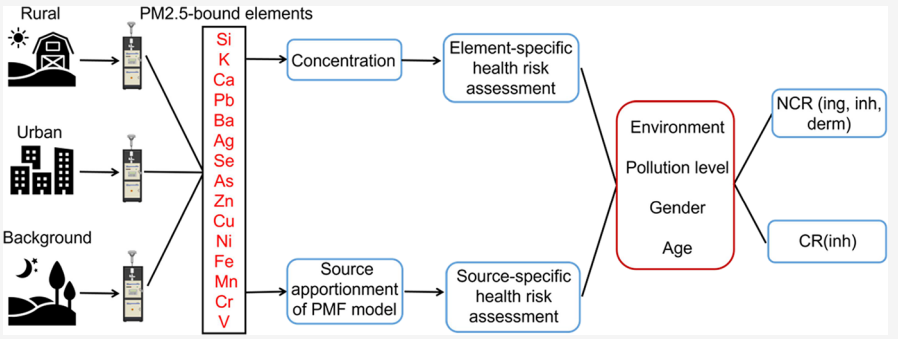

ABSTRACT: Key stages in people's lives have particular relevance for their health; the life-course approach stresses the importance of these stages. Here, we applied a life-course approach to analyze the health risks associated with $PM_{2.5}$-bound elements, which were measured at three sites with varying environmental conditions in eastern China. Road traffic was found to be the primary source of $PM_{2.5}$-bound elements at all three locations, but coal combustion was identified as the most important factor to induce both cancer risk (CR) and noncancer risk (NCR) across all age groups due to the higher toxicity of elements such as As and Pb associated with coal. Nearly half of NCR and over 90% of CR occurred in childhood (1−6 years) and adulthood (>18 years), respectively, and females have slightly higher NCR and lower CR than males. Rural population is found to be subject to the highest health risks. Synthesizing previous relevant studies and nationwide $PM_{2.5}$ concentration measurements, we reveal ubiquitous and large urban−rural environmental exposure disparities over China.

KEYWORDS: *life-course approach, road traffic, coal combustion, cancer risk (CR), noncancer risk (NCR)*

INTRODUCTION

Air pollution from $PM_{2.5}$ (particulate matter with an aerodynamic diameter less than 2.5 μm) is responsible for millions of premature deaths every year.[1,2] $PM_{2.5}$ mass concentration levels are currently used as environmental standards and have been steadily decreasing in China,[3,4] the United States,[5,6] and Europe[7,8] over the past decade. However, the global health burden of $PM_{2.5}$ pollution is still increasing annually.[9] $PM_{2.5}$ is a complex mixture of chemical constituents from various sources, and gathered evidence suggests that different chemical species associated with different emission sources may have different toxicity profiles.[10−15] This is particularly relevant to particulate elements such as Ni, Zn, Cu, Mn, Cd, Pb, Cr, and Fe.[11,16] They are emitted from both natural and anthropogenic sources (e.g., fugitive dust, coal combustion) and typically account for a few percentage of $PM_{2.5}$ mass, but they disproportionately lead to short-term or long-term adverse health effects, including pulmonary and heart diseases, and potentially premature death.[17,18]

$PM_{2.5}$-bound elements have long been considered trace components ("trace elements") and are mainly used to infer particulate sources.[19−23] Recently, in addition to toxicological studies, there has been increasing interest in linking human health risks with $PM_{2.5}$-bound element measurements to inform mitigation policies.[24−26] This is particularly true in China, where haze pollution featuring high $PM_{2.5}$ loadings continued to be a severe environmental and health concern in North China Plain, the Yangtze River Delta region, and the Pearl River Delta region.[27] For example, Huang et al.[25] characterized the concentration and fractionation of 14 elements in Beijing and concluded that traffic-related emission dominated the carcinogenic risk (CR) and noncarcinogenic

Received: July 9, 2023
Revised: October 28, 2023
Accepted: January 24, 2024
Published: February 14, 2024

risk (NCR) by $PM_{2.5}$-bound elements during low pollution days, while coal combustion becomes equally or even more important during moderate and severe pollution days. Another long-term continuous observation in Shenzhen, a megacity in Southern China, suggested the CR of five hazardous elements (Cd, Cr, Ni, Co, and Pb) in $PM_{2.5}$ showed a clear decreasing trend.[24,28]

Both offline and online analytical methods for airborne elements have their advantages and limitations. Offline methods, such as previous filter-based measurements, possess the potential to fractionate particulate elements into different bioavailable forms[25,26] and typically offer higher sensitivity, allowing for the detection of a broader range of elements compared to online techniques. However, it is important to acknowledge that offline methods, like the collection and analysis of 24-h integrated filters, come with labor-intensive processes, limited sample sizes that may not capture rapid pollution changes effectively,[29,30] and potential issues related to sampling artifacts and background residues.[31] Additionally, a crucial step in offline analysis involves acid digestion with a microwave digestion device, which, while effective, is not a nondestructive method and may yield variable element recoveries ranging from 60% to 130%.[24,25] Furthermore, previous research has predominantly been conducted in urban settings, potentially providing an incomplete picture of $PM_{2.5}$-bound elements in various environments. Importantly, the cumulative nature of $PM_{2.5}$-bound elements suggests that exposures may result in differing responses based on factors such as gender and age.[32,5,33] Therefore, it is critical to provide a full spectrum of the life-course health effects of $PM_{2.5}$-bound elements by gender and age.

In this study, we deployed three online analyzers for measuring $PM_{2.5}$-bound elements at three sites that are representative of background, rural, and urban environments in Eastern China (Figure S1). The sources of a full-year measurement of 15 elements were quantified using a positive matrix factorization (PMF) receptor model. The US Environmental Protection Agency (US EPA) human health risk assessment models were coupled with a life-course approach to evaluate the carcinogenic and noncarcinogenic health risks of these elements and their associated sources from multiple perspectives of environment, pollution level, gender, and age.

MATERIALS AND METHODS

The TOC art of this work illustrate the technical roadmap of our study. In brief, we conducted concentration observations of $PM_{2.5}$-bound elements at rural, urban, and background sites and identified their pollution sources. Based on this, we further assessed the health risks of heavy metals from both concentration-oriented and source-oriented perspectives. The following is a detailed description.

Field Measurements. Three sampling sites in Eastern China (Figures 1 and S1), namely, Dianshanhu (DH; 31.096°N, 120.988°E; 10 m a.g.l), Pudong (PD; 31.233°N, 121.545°E; 18 m a.g.l.), and Chongming (CM; 31.652°N, 121.426°E; 10 m a.g.l.), are included in this study. These sites are far from point sources and well representative of the rural, urban, and background environments. They are atmospheric flagship supersites and are strategically designed to distribute from SW to NE, perpendicular to the prevailing seasonal wind directions (NW during winter and SE during summer). We have conducted several field campaigns at these locations previously,[21,23,29] and the locations of these sites are shown in

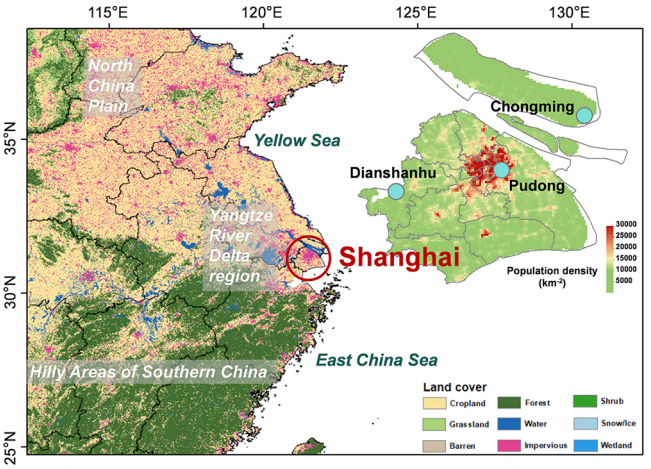

Figure 1. Locations of the sampling sites: Dianshanhu (DSH; rural), Pudong (PD; urban), and Chongming (CMD; background).

Figure S1 in Supporting Information (SI). For each site, from 1 January to 31 December 2019, hourly ambient mass concentrations of 15 elements (Si, K, Fe, Ca, Zn, Mn, Ba, Pb, Cu, Ag, As, Cr, Ni, V, and Se) in $PM_{2.5}$ were measured by a Xact multimetals monitor (Model Xact 625, Cooper Environmental Services LLT, OR, USA).[30] The high performance of the Xact metal analyzer in the determination of these elements has been vigorously validated in our method and application papers.[21,23,29] In brief, the Xact metal analyzer samples ambient air on the spooled Teflon filter tape at a flow rate of 16.7 L min^{-1} through the $PM_{2.5}$ cyclone inlet. The $PM_{2.5}$ deposits generated on the tape are automatically advanced to the analysis zone for nondestructive energy-dispersive X-ray fluorescence analysis to determine the concentrations of selected elemental species as the next sampling is initiated at a new tape spot. The 1 h time-resolution detection limits (in ng m^{-3}) are Si (17.80), K (1.17), Fe (0.17), Ca (0.30), Zn (0.23), Mn (0.14), Ba (0.39), Pb (0.13), Cu (0.27), Ag (1.90), As (0.11), Cr (0.12), Ni (0.10), V (0.12), and Se (0.14). The hourly mass concentrations of $PM_{2.5}$ were measured by a particulate monitor (Thermo, FH62C-14).

Source Apportionment. The receptor model, PMF, was used to identify and allocate the sources of measured $PM_{2.5}$-bound elements by employing a mass balance analysis while assuming mass conservation. The goal of this receptor model is to solve a specific equation and provide insights into the $PM_{2.5}$-bound elements:

$$x_{ij} = \sum_{k=1}^{p} g_{ij} \times f_{ij} + e_{ij} \quad (1)$$

Eq 1 involves measured concentrations x_{ij} of the j^{th} species in the i^{th} sample, contribution g_{ik} of the k^{th} source to the i^{th} sample, concentration f_{kj} of the j^{th} chemical species emitted by the k^{th} source, and residual element e_{ij} representing the PMF model error for species j measured in sample i. To solve eq 1, a Q function is defined and minimized. The Q function is expressed as follows:

$$Q = \sum_{i=1}^{n} \sum_{j=1}^{m} \left[\frac{e_{ij}}{\sigma_{ij}} \right]^2 \quad (2)$$

The equation involves the uncertainty (UNC) σ_{ij} associated with the j^{th} species in the i^{th} sample. Various Q functions can

https://doi.org/10.1021/acs.est.3c05404
Environ. Sci. Technol. 2024, 58, 3629−3640

be defined to solve the equation, such as Q_{true}, which includes all data, and Q_{robust}, which excludes outliers with scaled residuals (e_{ij}/σ_{ij}) greater than 4. To conduct our research, we utilized the US EPA PMF5.0, which can be downloaded at http://www.epa.gov/heasd/products/pmf/pmf.html.

Since particulate elements are mainly from primary emissions and the sample size of each element in our study is large, the relative and absolute contributions of different sources to their mass concentrations are particularly suitable to be quantified by PMF. The concentrations of measured elements and the measurement UNC of each element are the key inputs to run PMF. In this study, the concentrations and uncertainties of 15 $PM_{2.5}$-bound elements were included in the PMF5.0. If the concentration is less than or equal to the method detection limit (MDL) provided, the UNC is calculated by using the following equation:

$$\mathrm{UNC} = 5/6 \times \mathrm{MDL} \tag{3}$$

If the concentration is greater than the MDL, the UNC is then calculated as the detection limits (MDL) and a relative error (5%) summed in quadrature,

$$\mathrm{UNC} = \sqrt{(\mathrm{errorrate} \times \mathrm{massconcentration})^2 + (\mathrm{MDL})^2} \tag{4}$$

The model is a multivariate factor analysis and descriptive model, providing a solution that minimizes an objective function Q (Figure S2) based on UNC of each measurement. In this study, the PMF solutions from 3 to 6 factors were examined, and the five-factor solution is selected as it provides the most interpretable profiles and minimal Q value. In Table S1, we summarize the major marker species used to infer sources or factors. In this study, DSH (rural), PD (urban), and CMD (background) have similar origins, and we thus chose the same number of factors based on the PMF results. More details are described in Text S1 and Figures S2−S6.

Health Risk Assessment. The carcinogenic and NCRs from exposures of elements in $PM_{2.5}$ via various in vitro routes were calculated using US Environmental Protection Agency human health risk assessment model.[34,35] Exposure assessment and risk characterization are mainly involved in the model. Briefly, the elements included in the CR assessment are As, Cr, Ni, and Pb and those in the NCR assessment are As, Pb, Mn, V, Zn, Cr(VI), Cu, Ni, and Ba. First, we assess the NCR of elements by calculating the average daily dose (ADD) for three main pathways: ingestion (ing), inhalation (inh), and dermal absorption (derm)

$$C_{ing} = \frac{\mathrm{ADD} \times \mathrm{IngR} \times \mathrm{EF} \times \mathrm{ED}}{\mathrm{BW} \times \mathrm{AT}} \tag{5}$$

$$C_{inh} = \frac{\mathrm{ADD} \times \mathrm{InhR} \times \mathrm{EF} \times \mathrm{ED}}{\mathrm{BW} \times \mathrm{AT}} \tag{6}$$

$$C_{derm} = \frac{\mathrm{C} \times \mathrm{SA} \times \mathrm{CF} \times \mathrm{SL} \times \mathrm{ED} \times \mathrm{ED} \times \mathrm{ABS}}{\mathrm{BW} \times \mathrm{AT}} \tag{7}$$

where C is the concentration of elements (mg m^{-3} for inhalation or mg kg^{-1} for dermal absorption and ingestion). The concentrations for dermal absorption and ingestion were obtained by converting the atmospheric concentration (ng m^{-3}) and the mass concentration of $PM_{2.5}$ ($\mu g\ m^{-3}$). Cr(VI) was 1/7× the total Cr since the ratio of Cr(VI) to Cr(III) was reported to be approximately 1:6 (5). IngR is the ingestion rate (mg/day); EF is the exposure frequency (days); ED is the exposure duration (years); BW is the average body weight (kg); average time (AT) = ED × 365 days; InhR is the inhalation rate (m^3/day); SA is the exposed skin surface area (cm^2); CF is the conversion factor (kg/mg); SL is the skin adherence factor (mg/cm^2 × day); ABS is the skin absorption coefficient. Generic parameters (e.g., ED, CF, SL, and ABS) used in this study adopted the default values outlined in the EPA's Risk Assessment Guidance for Superfund Part B manual and fully integrated with the Chinese population exposure parameters (e.g., LT, InhR, IngR, and BW), as shown in Table S2. Since exposure parameters associated with ADD (e.g., InhR, BW, ED, IngR, etc.) vary with age, the NCR was assessed at different ages by eqs 5−7, respectively.

Second, the lifetime ADD for the inhalation exposure route is used to calculate element-specific CR. Finally, we analyzed the effects of NCR and CR of different pollution sources on human health by combining the results of PMF and health risk assessment. Importantly, several key exposure factors used in the model, such as inhalation rate, body weight, ingestion rate, and life expectancy are optimized specifically for the Chinese population (Table S2), which are adopted from the Exposure Factors Handbook of Chinese population issued by China's Ministry of Environmental Protection.[36] Details of the health risk assessment of $PM_{2.5}$-bound elements and emission sources are described in Texts S2 and S3, respectively.

RESULTS AND DISCUSSION

Concentrations and Sources. The 15 $PM_{2.5}$-bound elements (i.e., Si, K, Fe, Ca, Zn, Mn, Ba, Pb, Cu, Ag, As, Cr, Ni, V, and Se) included in our study have previously been frequently used to quantify source contributions and to assess health risks.[24,25] The daily data availabilities for all measured elements are satisfactory (>74%), and the average concentrations of these elements are shown in Tables S4−S6. We categorized the full-year measurement hours into low, moderate, and high pollution levels according to the Chinese national ambient air quality standard of 35 and 75 $\mu g\ m^{-3}$, that is, low pollution levels ($PM_{2.5} \le 35\ \mu g\ m^{-3}$), moderate pollution levels ($35 \le PM_{2.5} \le 75\ \mu g\ m^{-3}$), and high pollution levels ($PM_{2.5} \ge 75\ \mu g\ m^{-3}$). The daily mean concentrations of $PM_{2.5}$ (in $\mu g\ m^{-3}$) at rural, urban, and background sites were 42.6, 35.1, and 30.7, respectively, much higher than the WHO new air quality guidelines for daily mean $PM_{2.5}$ concentration (15 $\mu g\ m^{-3}$).

In Figure 2, we first compare and discuss the results on the concentrations and sources of elements by (rural, urban, or background) location and (low, moderate, or high $PM_{2.5}$) pollution level. Consistent with previous studies,[24,25] the total concentrations of all measured elements constituted 4.2% (2.0 $\mu g\ m^{-3}$), 3.7% (1.3 $\mu g\ m^{-3}$), and 3.4% (1.0 $\mu g\ m^{-3}$) of $PM_{2.5}$ mass at rural, urban, and background sites, respectively (see Table S9 for details). The concentrations of each measured element increase, while their overall contributions to $PM_{2.5}$ (percentage) decrease as pollution levels rise. Surprisingly, the rural elements were the highest in terms of both concentration and percentage, regardless of the pollution level. This can be partly explained by residential solid fuel combustion (RSFC) in rural China. Despite the promotion of clean energy (liquefied petroleum gas and electricity), biomass and coal are still widely used by farmers for cooking and heating.[37] The unreported residential coal consumption is 62% higher than that in official statistics.[38] RSFC emits large amounts of gaseous and particulate pollutants (including particulate

https://doi.org/10.1021/acs.est.3c05404
Environ. Sci. Technol. 2024, 58, 3629−3640

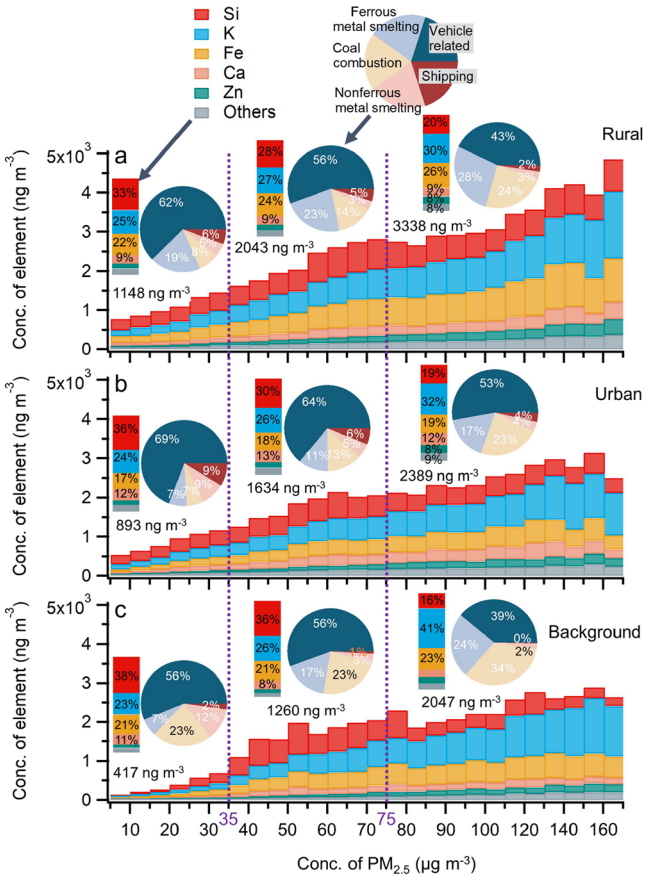

Figure 2. Variations in concentrations and sources of $PM_{2.5}$-bound elements at different $PM_{2.5}$ pollution levels in rural (a), urban (b), and background (a) locations. The bar chart indicates the proportion of various elements, while the pie chart illustrates the source contribution of the total $PM_{2.5}$-bound elements.

elements) in residential stoves due to low combustion efficiencies, which have been identified as the main source of haze pollution and health risks in China.[12,39,40]

For all sites, the top five most abundant elements are Si, K, Fe, Ca, and Zn, accounting for at least 90% of all measured elements (indicative of column stacked charts in Figure 2). However, their relative abundance varied considerably by pollution level; this is particularly true for Si and K. In particular, Si has the highest share at levels of low (33−38%) and moderate (28−36%) pollution. As the pollution level evolves from low to high, its share is gradually shrunk and crowded by K. Eventually, under the high pollution level, K jumps dramatically to take the largest share (30−41%), while Si recedes to the third place (16−20%) even after Fe (19−26%). As the most abundant element in the Earth's crust, ambient Si in Eastern China mostly comes from fugitive dust of road surfaces or construction fields,[29] thus its emissions should be seasonally consistent. Both element K and nonsea salt K ion (nss-K^+) are chemical tracers of biomass burning.[41,42] Therefore, the explosive increase in K during heavy pollution periods reflects more intensive biomass burning for winter heating, echoing the above discussion on the importance of RSFC to China's winter haze pollution.

At each site, the total measured elements can be apportioned by the PMF receptor model to five emission sources (Text S1 and Figure S5). As shown in the pie charts in Figure 2, irrespective of location or pollution level, traffic-related emissions are the dominant contributor, especially in urban areas (53−69%). However, their shares continue to shrink as pollution worsens, in line with trends of shipping and nonferrous metal smelting. In most cases, shipping is a minor source of elements, decreasing in proportion as pollution increases, accounting on average for 5, 7, and 2% of the total elements at rural, urban, and background sites. Ferrous metal smelting is generally the second largest source at nonurban sites and its share increases dramatically from low to high pollution levels at sites of rural (from 19 to 28%), urban (from 7 to 17%), and background (from 7 to 24%). The mean contribution of coal combustion is 18, 12, and 23% at rural, urban, and background sites, and its share at all sites increases as pollution level rise. Most typically, at background site, its share (34%) is comparable to that of vehicle-related emissions (39%) at high pollution level. Overall, nonferrous metal smelting is a small source at all sites (<10%) but can reach up to 12% at background site during low pollution period.

Element-Induced Health Risks. In this section, we discuss element-specific NCR and CR over the life course by age, gender, and pollution level. Despite higher NCR and CR at rural site due to much higher elemental loadings, the sites of rural, urban, and background have basically the same pattern of element-specific NCRs (Figure S7) and CRs (Figure S8). More specifically, the relative proportions of NCR (or CR) caused by various elements do not differ significantly across sites. Therefore, here we focus on the results of rural site as an example. In our study, the entire life span is divided into 17 age groups, and their health risks are calculated separately. To facilitate discussion, we reclassify the life course into four key stages, namely infancy (0−12 months), childhood (1−6 years), adolescence (7−18 years), and adulthood (>18 years). In Figure 3, females have slightly higher NCR and lower CR, which can be explained by the lower body weight and the smaller inhalation rate used to calculate the NCR and CR in females (Text S2), respectively. Given that the gender differences in health risks are not significant, all genders are included when referring to NCR or CR thereafter.

In Figure 3, the top-four (As, Mn, Pb, and V) and top-two (As and Cr(VI)) elements jointly contribute to at least 91 and 96% of NCR and CR at different pollution levels. As and Mn, which are often associated with coal combustion, were also been identified as the elements with the highest NCR in Beijing (Northern China)[25] and Shenzhen (Southern China),[24] respectively. In our study, except in adulthood, the NCR of As alone can exceed the safety limit (i.e., hazard quotient or HQ = 1).[24,25] The NCR of Mn and Pb is also generally above 1 in childhood and adolescence. Regardless of age, gender, or pollution level, all of the NCR induced by total measured elements are all over 1. Moreover, on average, the total (accumulative) NCR at low, moderate, and high pollution levels are 3.5, 3.7, and 4.4, respectively, indicating a ubiquitously high occurrence probability of adverse non-carcinogenic effects in the rural population. For CR, the minimum risk value or an acceptable level is 1.0×10^{-6}, which means that one excess cancer case in a population of one million people could potentially occur. High CR ($>1.0 \times 10^{-5}$) can only be observed during adulthood, accounting for most of the carcinogenic effects (89% on average). This suggests the accumulative nature of elements to induce cancer effects.

From low to high pollution levels, among the major elements, only the relative contributions of Mn-induced NCRs (from 16 to 39%) and As-induced CRs (from 69 to

https://doi.org/10.1021/acs.est.3c05404
Environ. Sci. Technol. 2024, 58, 3629−3640

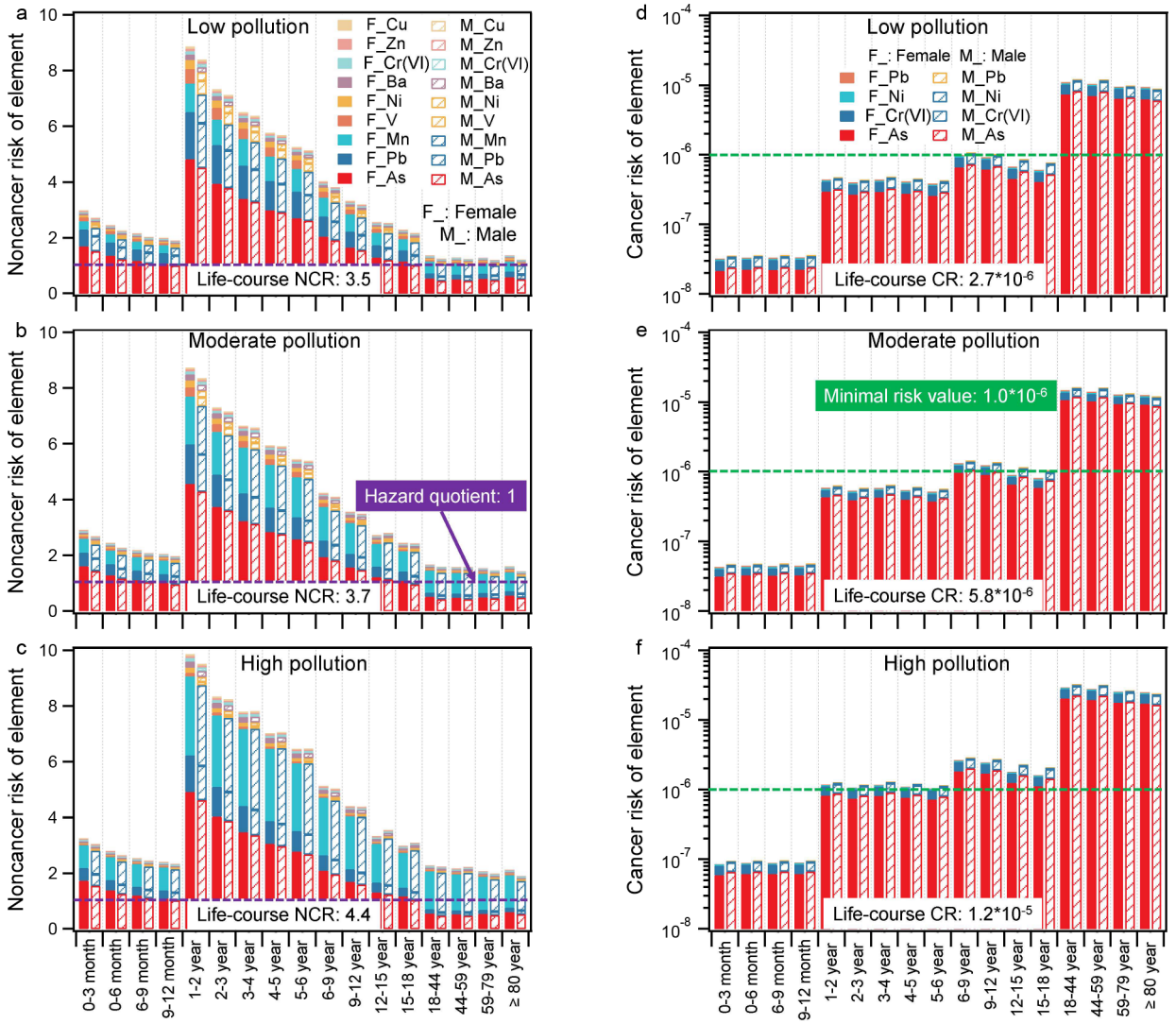

Figure 3. Element-specific health risks by age, gender, and $PM_{2.5}$ pollution level at rural site. (a–c) NCR at low, moderate, and high pollution levels, respectively. (d–f) CR at low, moderate, and high pollution levels, respectively. For each subfigure with two pie charts, the top pie chart and the bottom pie chart represent the proportion of each age group for female and male categories, respectively.

74%) increase. As to the total measured elements, unlike the rapid increase in absolute concentrations (Figure 1) and life-course CRs (right panel of Figure 3), the increase in life-course NCRs is not significant (left panel of Figure 3). There are three (ingestion, inhalation, and dermal absorption) and one (inhalation) exposure pathways for NCR and CR, respectively (Text S2). The ADD from the routes of ingestion and dermal absorption are 3 and 1 order of magnitude higher than inhalation (Table S2). Different from inhalation, the former two are determined by the ratio of element versus $PM_{2.5}$ concentration. The general lower [element/$PM_{2.5}$] under higher pollution periods could therefore offset the influence of increased concentration to NCR.

From young to old age, the relative contributions of major elements to both NCR and CR remain stable (Figure 3). However, the absolute values of NCR and CR fluctuate with age group. The most obvious example is the sudden increase in NCR and CR when age reaches 1 and 18 years, respectively, both of which can be largely attributed to changes in the assignment of exposure duration (ED). ED is a key exposure parameter in the US EPA health risk model. Since the subgroup gap for the pre- and post-1 year age groups is 0.25 and 1 year, respectively, the ED used to calculate NCR and CR for population over 1 year is four times greater than that for population under 1 year. Moreover, for CR, according to the US EPA, the ED before the age of 18 is the corresponding age group, which is relatively small. While after adulthood, 49 years is uniformly designated as the ED in the model to calculate CR.

Source-Oriented Health Risks. In combination with the source profiles resolved by PMF, the element-specific health risk is then translated into the source-oriented health risk (Text S3). To facilitate the translation of science into source-oriented control actions effectively, in the main text, we focus on source-oriented health risks from year-round averaged source apportionment results. For results on source-oriented NCR and CR at different pollution levels, one can refer to Figures S9 and S10, respectively.

In Figure 4, we report the full-year source-oriented NCR and CR for each site over four different key life stages. Below, we summarize the main findings in a nutshell.

https://doi.org/10.1021/acs.est.3c05404
Environ. Sci. Technol. 2024, 58, 3629–3640

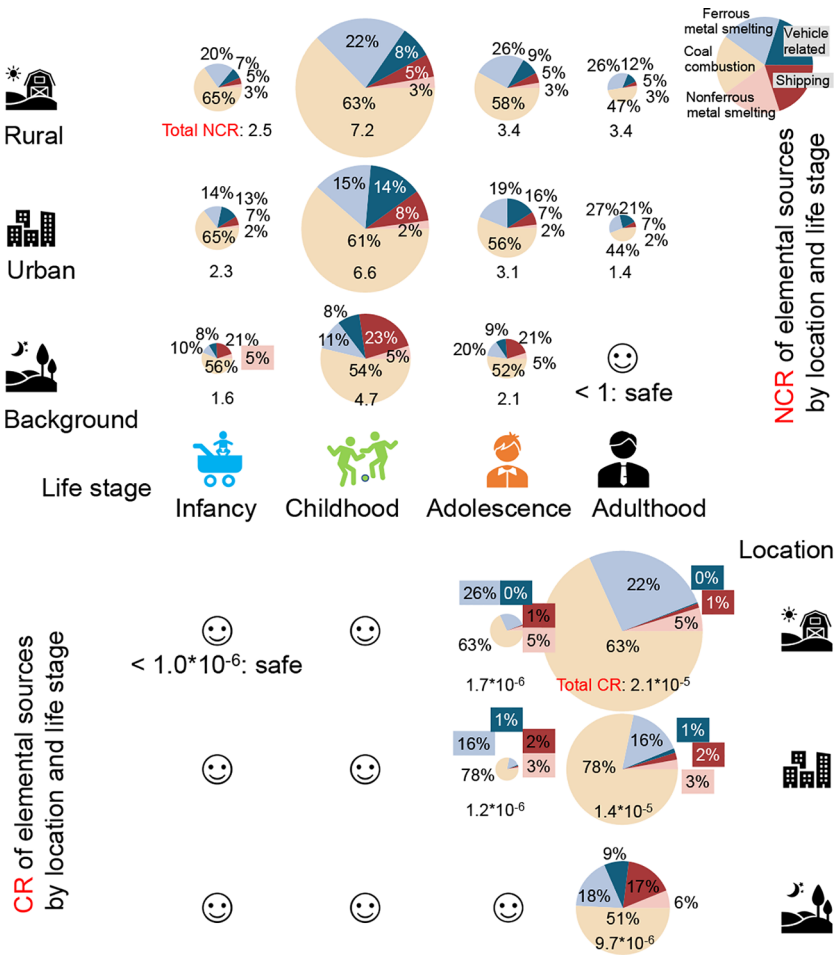

Figure 4. Source-oriented health risks by life stage and location. Top: NCR; bottom: CR. The size of each section of the pie chart indicates the level of risk, and the numbers below the chart indicate the absolute health risk values for NCR and CR.

(1) Coal combustion, not traffic-emitted emissions, should be prioritized for control. Overall, traffic-emitted emissions account for 50, 64, and 52% of the total mass concentrations of elements at rural, urban, and background sties, respectively, which is much higher than coal combustion (<20% on average). However, vehicle-related emissions mainly produce nonexhaust elements such as Ca, Fe, K and Si, which are commonly found in the natural atmosphere and are less hazardous to human health.[25] In contrast, coal combustion disproportionately contributes to 50−60 and 60−70% of NCR and CR throughout the life span. This is mainly because nearly half of NCR and over 70% of CR is contributed by As, and most of As at rural (93%), urban (97%), and background (65%) sites are derived from coal combustion.

(2) NCR and CR occur mainly in the stages of childhood and adulthood, respectively. For NCR, except in adulthood at the background site, all NCR are greater than 1, irrespective of location and life stage. However, ranging from 4.7 to 7.2, NCR in childhood is particularly high, taking up 44, 49, and 51% of the accumulative NCR at rural, urban, and background sites. Given that childhood (1−6 years) is a very early stage of life, excessive NCR will have serious health implications throughout the life course. Therefore, control measures should specifically target the main sources driving NCR in childhood. For CR, most CR occurs in adulthood, and the average CR at the three sites is nearly 15 times higher than the safety limit.

(3) Region-specific and multisource control measures are required at the current stage. As mentioned earlier, coal combustion is the number one source of health risks. However, currently, even with a total ban on coal combustion, the locations and life stages of previously exceeded safety limits in Figure 4 remain largely unchanged. In fact, China is ahead of most countries in pollution control of coal-fired power plants (CFPPs),[43] thus the potential for emission reduction from CFPPs has largely peaked.[44] Other sources such as ferrous metal smelting also need to be particularly controlled, as it alone can cause NCR in childhood and CR in adulthood to exceed the safety limits. In addition, effective reductions in vehicle-related and shipping emissions have significant health benefits in urban and background areas, respectively.

(4) From Figures S11 to S17, we have extensively investigated the seasons during which individuals in rural, urban, or background settings are most susceptible to heightened concentrations from specific emission sources. Our analysis reveals pronounced variations in $PM_{2.5}$ elements over different seasons, shedding light on the heightened exposure of rural populations during the winter season. This exposure has been attributed to escalated coal and biomass-burning activities.

Evidence of Large Urban−Rural Health Inequity. Irrespective of life stage, Figure 4 shows that both NCR and CR are higher at the rural site than at urban and background sites. In eastern China, with an average share of ∼18% in

https://doi.org/10.1021/acs.est.3c05404
Environ. Sci. Technol. 2024, 58, 3629−3640

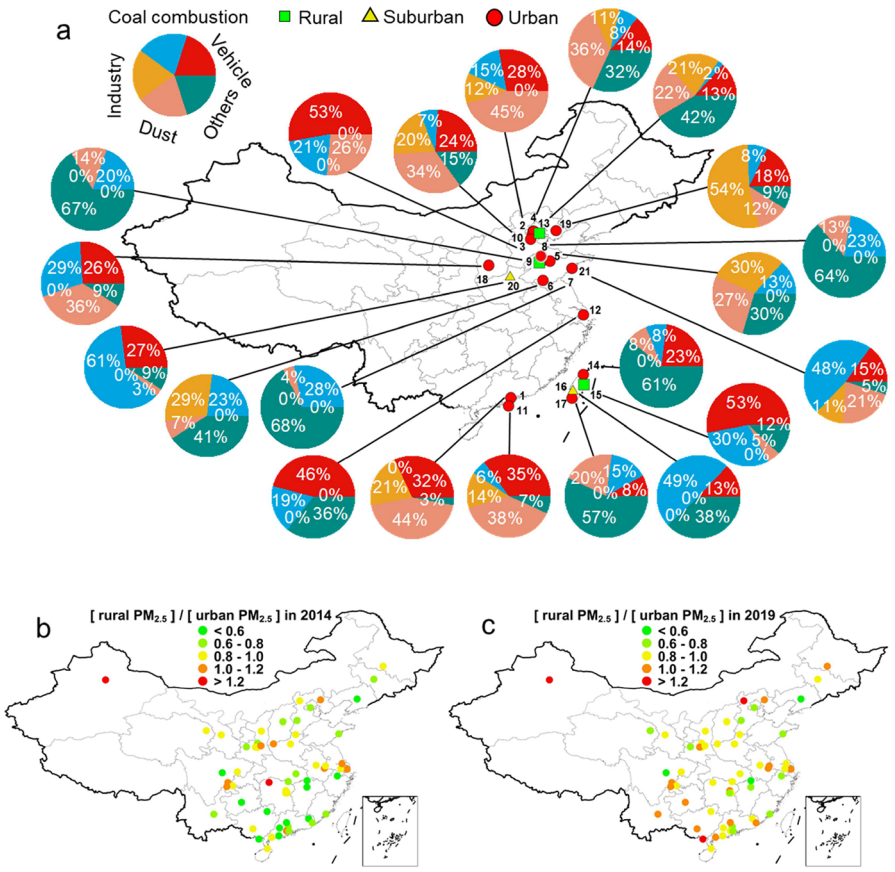

Figure 5. (a) Compilation of previous studies (see Table S7) on the source apportionment of particulate elements in China. Ratios of rural annual $PM_{2.5}$ concentration versus urban annual $PM_{2.5}$ concentration (i.e., [rural $PM_{2.5}$]/[urban $PM_{2.5}$]) for 57 cities in China in 2014 (b) and 2019 (c) (see Table S8).

$PM_{2.5}$-bound elements, coal combustion is responsible for about 60% of health risks. Eastern China is not special, as previous studies have shown a ubiquitous contribution of coal combustion to particulate elements across China (21% on average; Figure 5a). Consistent with the key regions of China's air pollution control, these studies have concentrated on urban environments in Eastern China (Table S7), lacking a full understanding of rural areas and the whole nation. Given the unique presence of residential coal combustion in rural China and its disproportionately large contribution to health risks,[12,37,39,40,43] this is likely to give rise to rural exposure disparities.

China currently operates nearly 2000 air quality monitoring stations throughout the nation and publicly releases hourly concentrations of major pollutants like $PM_{2.5}$.[4,45] Although they exclude particulate elements, very few of these sites are set in rural environments (Figures 4b and 5a5), which provides an opportunity to examine exposure disparity caused by urban−rural differences in particulate pollution on a national scale. Here, annual $PM_{2.5}$ concentrations in 2014 and 2019 are extracted from 57 paired rural and urban stations (Table S8). We are fully aware that high $PM_{2.5}$ does not imply high and toxic elemental content, and in fact varies considerably from region to region (Figure 5a). Nevertheless, their [rural $PM_{2.5}$]/[urban $PM_{2.5}$] ratio can be tentatively used as an indicator of testing rural exposure disparity from particulate pollution. If the ratio for a given city is greater than 1, then there is rural environmental inequity, and the larger the ratio, the more severe the inequity.

Taking the 57 cities as a whole, the annual average concentration of $PM_{2.5}$ in 2014 (49.6 $\mu g\ m^{-3}$; Figure 5b) is much higher than that in 2019 (38.0 $\mu g\ m^{-3}$; Figure 5c). This confirms that $PM_{2.5}$ pollution in China has been improved substantially, while the improvement is unbalanced between urban (from 54.5 to 44.6 $\mu g\ m^{-3}$) and rural (from 40 to 36 $\mu g\ m^{-3}$). The reduction in rural $PM_{2.5}$ (10.0%) is much smaller than that in urban $PM_{2.5}$ (18.2%), suggesting that rural disparities of environmental health are widening in China. Indeed, of the 57 cities, 11 had a [rural $PM_{2.5}$]/[urban $PM_{2.5}$] ratio greater than 1 in 2014 (Figure 5b), which increased to 18 in 2019 (Figure 5c). Although $PM_{2.5}$ remains higher in most urban areas than in rural areas, the continued expansion of rural $PM_{2.5}$ inequity may lead to greater rural health inequity, given the large contribution of residential coal combustion to rural $PM_{2.5}$.[39]

In summary, we provide a full spectrum of concentration- and source-associated health risks from multiroute exposures of $PM_{2.5}$-bound elements over the life course in Eastern China. What makes our research stand out including field measurements and health risk analysis. Experimentally, a full-year time-revolved measurements of 15 elements in rural, urban, and background locations are used to yield robust source apportionment results in various environments. Meanwhile, many key factors used in health assessment are obtained from localized studies to be optimized for the Chinese population. These multifaceted results provide valuable information for the development of source-oriented control strategies to effectively reduce the health risks of particulate elements to susceptible

https://doi.org/10.1021/acs.est.3c05404
Environ. Sci. Technol. 2024, 58, 3629−3640

populations. Importantly, we provide evidence of large urban−rural disparity from particulate pollution in China. We argue that the continuous ignorance of air quality control in rural China could further enhance rural environmental health inequities in the future. Notwithstanding, there are two major limitations in our study. First, many other important toxic constituents in $PM_{2.5}$, such as polycyclic aromatic hydrocarbons and elemental carbon,[10−12,15] are not considered. Second, our health assessments were based on external exposure concentrations but ignored bioaccessibility and bioaccumulation; they therefore cannot quantify actual amounts of chemicals absorbed into the human body and may overestimate or underestimate the risk.[26] Third, although our study primarily focused on assessing the health risks associated with exposure to trace elements, we recognize the importance of secondary aerosols in air quality research. The potential health implications of secondary aerosol formation represent an essential area for further investigation. The last but not least, our use of 1 year measurements to estimate long-term health risks is a practical approach given the available data, but it does introduce uncertainties. We understand that causally linking short-term exposures to long-term health outcomes, particularly in the context of childhood exposure, is a complex endeavor. Therefore, we emphasize that our risk assessment framework provides valuable insights into the potential hazards associated with current pollution levels and offers guidance for targeted interventions. While we cannot definitively establish direct causal links, our study serves as a starting point for further research and discussions on the complex relationships between air pollution and public health. As more comprehensive and long-term data become available, we encourage future investigations to refine these risk estimates and strengthen the evidence base for informed decision-making.

■ ASSOCIATED CONTENT

Data Availability Statement

All data supporting the conclusions are included in the article and Supporting Information. Readers can access and download the data obtained from Pudong site freely through the following link: https://zenodo.org/doi/10.5281/zenodo.10048729. Additional data are available upon request.

Supporting Information

The Supporting Information is available free of charge at https://pubs.acs.org/doi/10.1021/acs.est.3c05404.

Source apportionment of $PM_{2.5}$-bound elements by PMF model; element-specific health risk assessment; source-specific health risk assessment; field photos of the sampling sites; Q/Q_{exp} values varied with a number of factors resolved by PMF; different source profiles obtained by PMF; element- or source-specific NCR or CR by location, age, gender, and pollution level; health risks of $PM_{2.5}$ elements and associated sources in different locations and seasons; major marker elements in the five sources of PMF; exposure parameters used for health risk assessment; exposure dose−response parameters; statistics of $PM_{2.5}$-bound elements in different locations; compilation of previous source apportionment studies of particulate elements in China; urban and rural $PM_{2.5}$ concentrations and their ratios for 57 sites in China in 2014 and 2019; relative and absolute values of the total $PM_{2.5}$-bound element concentrations and different sources at rural, urban, and background sites (PDF)

■ AUTHOR INFORMATION

Corresponding Author

Yunhua Chang − *Collaborative Innovation Center on Forecast and Evaluation of Meteorological Disasters, NUIST Center on Atmospheric Environment, Nanjing University of Information Science & Technology (NUIST), Nanjing 210044, China;* orcid.org/0000-0002-1622-5330; Phone: +86-25-15189823369; Email: changy13@nuist.edu.cn; Fax: +86-25-58731193

Authors

Kai Cheng − *Collaborative Innovation Center on Forecast and Evaluation of Meteorological Disasters, NUIST Center on Atmospheric Environment, Nanjing University of Information Science & Technology (NUIST), Nanjing 210044, China*

Xuhui Lee − *School of Forestry and Environmental Studies, Yale University, New Haven, Connecticut 06511, United States*

Dongsheng Ji − *State Key Laboratory of Atmospheric Boundary Layer Physics and Atmospheric Chemistry, Institute of Atmospheric Physics, Chinese Academy of Sciences, Beijing 100029, China;* orcid.org/0000-0002-7889-4417

Liping Qiao − *State Environmental Protection Key Laboratory of Formation and Prevention of Urban Air Pollution Complex, Shanghai Academy of Environmental Sciences, Shanghai 200233, China*

Zhong Zou − *Department of Environmental Science and Engineering, Shanghai Key Laboratory of Atmospheric Particle Pollution and Prevention, Fudan University, Shanghai 200433, China*

Yusheng Duan − *Shanghai Environmental Monitoring Center, Shanghai 200030, China*

Ru-Jin Huang − *State Key Laboratory of Loess and Quaternary Geology, Center for Excellence in Quaternary Science and Global Change, and Key Laboratory of Aerosol Chemistry and Physics, Institute of Earth and Environment, Chinese Academy of Sciences, Xi'an 710061, China;* orcid.org/0000-0002-4907-9616

Complete contact information is available at: https://pubs.acs.org/10.1021/acs.est.3c05404

Author Contributions

Y.C. designed and led the study. Y.C. and K.C. performed the research and wrote the draft. X.L., D.J., L.Q., Z.Z., Y.D., and R.H. discussed the results and analysis. All authors commented on the manuscript.

Notes

The authors declare no competing financial interest.

■ ACKNOWLEDGMENTS

This work was supported by the National Natural Science Foundation of China (Grant No. 41975166) and the Jiangsu Natural Science Fund for Excellent Young Scholars (Grant No. BK20211594).

■ REFERENCES

(1) Stanaway, J. D.; Afshin, A.; Gakidou, E.; Lim, S. S.; Abate, D.; Abate, K. H.; Abbafati, C.; Abbasi, N.; Abbastabar, H.; Abd-Allah, F.;

Abdela, J.; Abdelalim, A.; Abdollahpour, I.; Abdulkader, R. S.; Abebe, M.; Abebe, Z.; Abera, S. F.; Abil, O. Z.; Abraha, H. N.; Abrham, A. R.; Abu-Raddad, L. J.; Abu-Rmeileh, N. M. E.; Accrombessi, M. M. K.; Acharya, D.; Acharya, P.; Adamu, A. A.; Adane, A. A.; Adebayo, O. M.; Adedoyin, R. A.; Adekanmbi, V.; Ademi, Z.; Adetokunboh, O. O.; Adib, M. G.; Admasie, A.; Adsuar, J. C.; Afanvi, K. A.; Afarideh, M.; Agarwal, G.; Aggarwal, A.; Aghayan, S. A.; Agrawal, A.; Agrawal, S.; Ahmadi, A.; Ahmadi, M.; Ahmadieh, H.; Ahmed, M. B.; Aichour, A. N.; Aichour, I.; Aichour, M. T. E.; Akbari, M. E.; Akinyemiju, T.; Akseer, N.; Al-Aly, Z.; Al-Eyadhy, A.; Al-Mekhlafi, H. M.; Alahdab, F.; Alam, K.; Alam, S.; Alam, T.; Alashi, A.; Alavian, S. M.; Alene, K. A.; Ali, K.; Ali, S. M.; Alijanzadeh, M.; Alizadeh-Navaei, R.; Aljunid, S. M.; Alkerwi, A. A.; Alla, F.; Alsharif, U.; Altirkawi, K.; Alvis-Guzman, N.; Amare, A. T.; Ammar, W.; Anber, N. H.; Anderson, J. A.; Andrei, C. L.; Androudi, S.; Animut, M. D.; Anjomshoa, M.; Ansha, M. G.; Antó, J. M.; Antonio, C. A. T.; Anwari, P.; Appiah, L. T.; Appiah, S. C. Y.; Arabloo, J.; Aremu, O.; Ärnlöv, J.; Artaman, A.; Aryal, K. K.; Asayesh, H.; Ataro, Z.; Ausloos, M.; Avokpaho, E. F. G. A.; Awasthi, A.; Ayala Quintanilla, B. P.; Ayer, R.; Ayuk, T. B.; Azzopardi, P. S.; Babazadeh, A.; Badali, H.; Badawi, A.; Balakrishnan, K.; Bali, A. G.; Ball, K.; Ballew, S. H.; Banach, M.; Banoub, J. A. M.; Barac, A.; Barker-Collo, S. L.; Bärnighausen, T. W.; Barrero, L. H.; Basu, S.; Baune, B. T.; Bazargan-Hejazi, S.; Bedi, N.; Beghi, E.; Behzadifar, M.; Behzadifar, M.; Béjot, Y.; Bekele, B. B.; Bekru, E. T.; Belay, E.; Belay, Y. A.; Bell, M. L.; Bello, A. K.; Bennett, D. A.; Bensenor, I. M.; Bergeron, G.; Berhane, A.; Bernabe, E.; Bernstein, R. S.; Beuran, M.; Beyranvand, T.; Bhala, N.; Bhalla, A.; Bhattarai, S.; Bhutta, Z. A.; Biadgo, B.; Bijani, A.; Bikbov, B.; Bilano, V.; Bililign, N.; Bin Sayeed, M. S.; Bisanzio, D.; Biswas, T.; Bjørge, T.; Blacker, B. F.; Bleyer, A.; Borschmann, R.; Bou-Orm, I. R.; Boufous, S.; Bourne, R.; Brady, O. J.; Brauer, M.; Brazinova, A.; Breitborde, N. J. K.; Brenner, H.; Briko, A. N.; Britton, G.; Brugha, T.; Buchbinder, R.; Burnett, R. T.; Busse, R.; Butt, Z. A.; Cahill, L. E.; Cahuana-Hurtado, L.; Campos-Nonato, I. R.; Cárdenas, R.; Carreras, G.; Carrero, J. J.; Carvalho, F.; Castañeda-Orjuela, C. A.; Castillo Rivas, J.; Castro, F.; Catalá-López, F.; Causey, K.; Cercy, K. M.; Cerin, E.; Chaiah, Y.; Chang, H.-Y.; Chang, J.-C.; Chang, K.-L.; Charlson, F. J.; Chattopadhyay, A.; Chattu, V. K.; Chee, M. L.; Cheng, C.-Y.; Chew, A.; Chiang, P. P.-C.; Chimed-Ochir, O.; Chin, K. L.; Chitheer, A.; Choi, J.-Y. J.; Chowdhury, R.; Christensen, H.; Christopher, D. J.; Chung, S.-C.; Cicuttini, F. M.; Cirillo, M.; Cohen, A. J.; Collado-Mateo, D.; Cooper, C.; Cooper, O. R.; Coresh, J.; Cornaby, L.; Cortesi, P. A.; Cortinovis, M.; Costa, M.; Cousin, E.; Criqui, M. H.; Cromwell, E. A.; Cundiff, D. K.; Daba, A. K.; Dachew, B. A.; Dadi, A. F.; Damasceno, A. A. M.; Dandona, L.; Dandona, R.; Darby, S. C.; Dargan, P. I.; Daryani, A.; Das Gupta, R.; Das Neves, J.; Dasa, T. T.; Dash, A. P.; Davitoiu, D. V.; Davletov, K.; De La Cruz-Góngora, V.; De La Hoz, F. P.; De Leo, D.; De Neve, J.-W.; Degenhardt, L.; Deiparine, S.; Dellavalle, R. P.; Demoz, G. T.; Denova-Gutiérrez, E.; Deribe, K.; Dervenis, N.; Deshpande, A.; Des Jarlais, D. C.; Dessie, G. A.; Deveber, G. A.; Dey, S.; Dharmaratne, S. D.; Dhimal, M.; Dinberu, M. T.; Ding, E. L.; Diro, H. D.; Djalalinia, S.; Do, H. P.; Dokova, K.; Doku, D. T.; Doyle, K. E.; Driscoll, T. R.; Dubey, M.; Dubljanin, E.; Duken, E. E.; Duncan, B. B.; Duraes, A. R.; Ebert, N.; Ebrahimi, H.; Ebrahimpour, S.; Edvardsson, D.; Effiong, A.; Eggen, A. E.; El Bcheraoui, C.; El-Khatib, Z.; Elyazar, I. R.; Enayati, A.; Endries, A. Y.; Er, B.; Erskine, H. E.; Eskandarieh, S.; Esteghamati, A.; Estep, K.; Fakhim, H.; Faramarzi, M.; Fareed, M.; Farid, T. A.; Farinha, C. S. E. S.; Farioli, A.; Faro, A.; Farvid, M. S.; Farzaei, M. H.; Fatima, B.; Fay, K. A.; Fazaeli, A. A.; Feigin, V. L.; Feigl, A. B.; Fereshtehnejad, S.-M.; Fernandes, E.; Fernandes, J. C.; Ferrara, G.; Ferrari, A. J.; Ferreira, M. L.; Filip, I.; Finger, J. D.; Fischer, F.; Foigt, N. A.; Foreman, K. J.; Fukumoto, T.; Fullman, N.; Fürst, T.; Furtado, J. M.; Futran, N. D.; Gall, S.; Gallus, S.; Gamkrelidze, A.; Ganji, M.; Garcia-Basteiro, A. L.; Gardner, W. M.; Gebre, A. K.; Gebremedhin, A. T.; Gebremichael, T. G.; Gelano, T. F.; Geleijnse, J. M.; Geramo, Y. C. D.; Gething, P. W.; Gezae, K. E.; Ghadimi, R.; Ghadiri, K.; Ghasemi Falavarjani, K.; Ghasemi-Kasman, M.; Ghimire, M.; Ghosh, R.; Ghoshal, A. G.; Giampaoli, S.; Gill, P. S.; Gill, T. K.; Gillum, R. F.; Ginawi, I. A.; Giussani, G.; Gnedovskaya, E. V.; Godwin, W. W.; Goli, S.; Gómez-Dantés, H.; Gona, P. N.; Gopalani, S. V.; Goulart, A. C.; Grada, A.; Grams, M. E.; Grosso, G.; Gugnani, H. C.; Guo, Y.; Gupta, R.; Gupta, R.; Gupta, T.; Gutiérrez, R. A.; Gutiérrez-Torres, D. S.; Haagsma, J. A.; Habtewold, T. D.; Hachinski, V.; Hafezi-Nejad, N.; Hagos, T. B.; Hailegiyorgis, T. T.; Hailu, G. B.; Haj-Mirzaian, A.; Haj-Mirzaian, A.; Hamadeh, R. R.; Hamidi, S.; Handal, A. J.; Hankey, G. J.; Hao, Y.; Harb, H. L.; Harikrishnan, S.; Haro, J. M.; Hassankhani, H.; Hassen, H. Y.; Havmoeller, R.; Hawley, C. N.; Hay, S. I.; Hedayatizadeh-Omran, A.; Heibati, B.; Heidari, B.; Heidari, M.; Hendrie, D.; Henok, A.; Heredia-Pi, I.; Herteliu, C.; Heydarpour, F.; Heydarpour, S.; Hibstu, D. T.; Higazi, T. B.; Hilawe, E. H.; Hoek, H. W.; Hoffman, H. J.; Hole, M. K.; Homaie Rad, E.; Hoogar, P.; Hosgood, H. D.; Hosseini, S. M.; Hosseinzadeh, M.; Hostiuc, M.; Hostiuc, S.; Hoy, D. G.; Hsairi, M.; Hsiao, T.; Hu, G.; Hu, H.; Huang, J. J.; Hussen, M. A.; Huynh, C. K.; Iburg, K. M.; Ikeda, N.; Ilesanmi, O. S.; Iqbal, U.; Irvani, S. S. N.; Irvine, C. M. S.; Islam, S. M. S.; Islami, F.; Jackson, M. D.; Jacobsen, K. H.; Jahangiry, L.; Jahanmehr, N.; Jain, S. K.; Jakovljevic, M.; James, S. L.; Jassal, S. K.; Jayatilleke, A. U.; Jeemon, P.; Jha, R. P.; Jha, V.; Ji, J. S.; Jonas, J. B.; Jonnagaddala, J.; Jorjoran Shushtari, Z.; Joshi, A.; Jozwiak, J. J.; Jürisson, M.; Kabir, Z.; Kahsay, A.; Kalani, R.; Kanchan, T.; Kant, S.; Kar, C.; Karami, M.; Karami Matin, B.; Karch, A.; Karema, C.; Karimi, N.; Karimi, S. M.; Kasaeian, A.; Kassa, D. H.; Kassa, G. M.; Kassa, T. D.; Kassebaum, N. J.; Katikireddi, S. V.; Kaul, A.; Kawakami, N.; Kazemi, Z.; Karyani, A. K.; Kefale, A. T.; Keiyoro, P. N.; Kemp, G. R.; Kengne, A. P.; Keren, A.; Kesavachandran, C. N.; Khader, Y. S.; Khafaei, B.; Khafaie, M. A.; Khajavi, A.; Khalid, N.; Khalil, I. A.; Khan, G.; Khan, M. S.; Khan, M. A.; Khang, Y.-H.; Khater, M. M.; Khazaei, M.; Khazaie, H.; Khoja, A. T.; Khosravi, A.; Khosravi, M. H.; Kiadaliri, A. A.; Kiirithio, D. N.; Kim, C.-I.; Kim, D.; Kim, Y.-E.; Kim, Y. J.; Kimokoti, R. W.; Kinfu, Y.; Kisa, A.; Kissimova-Skarbek, K.; Kivimäki, M.; Knibbs, L. D.; Knudsen, A. K. S.; Kochhar, S.; Kokubo, Y.; Kolola, T.; Kopec, J. A.; Kosen, S.; Koul, P. A.; Koyanagi, A.; Kravchenko, M. A.; Krishan, K.; Krohn, K. J.; Kromhout, H.; Kuate Defo, B.; Kucuk Bicer, B.; Kumar, G. A.; Kumar, M.; Kuzin, I.; Kyu, H. H.; Lachat, C.; Lad, D. P.; Lad, S. D.; Lafranconi, A.; Lalloo, R.; Lallukka, T.; Lami, F. H.; Lang, J. J.; Lansingh, V. C.; Larson, S. L.; Latifi, A.; Lazarus, J. V.; Lee, P. H.; Leigh, J.; Leili, M.; Leshargie, C. T.; Leung, J.; Levi, M.; Lewycka, S.; Li, S.; Li, Y.; Liang, J.; Liang, X.; Liao, Y.; Liben, M. L.; Lim, L.-L.; Linn, S.; Liu, S.; Lodha, R.; Logroscino, G.; Lopez, A. D.; Lorkowski, S.; Lotufo, P. A.; Lozano, R.; Lucas, T. C. D.; Lunevicius, R.; Ma, S.; Macarayan, E. R. K.; Machado, Í. E.; Madotto, F.; Mai, H. T.; Majdan, M.; Majdzadeh, R.; Majeed, A.; Malekzadeh, R.; Malta, D. C.; Mamun, A. A.; Manda, A.-L.; Manguerra, H.; Mansournia, M. A.; Mantovani, L. G.; Maravilla, J. C.; Marcenes, W.; Marks, A.; Martin, R. V.; Martins, S. C. O.; Martins-Melo, F. R.; März, W.; Marzan, M. B.; Massenburg, B. B.; Mathur, M. R.; Mathur, P.; Matsushita, K.; Maulik, P. K.; Mazidi, M.; McAlinden, C.; McGrath, J. J.; McKee, M.; Mehrotra, R.; Mehta, K. M.; Mehta, V.; Meier, T.; Mekonnen, F. A.; Melaku, Y. A.; Melese, A.; Melku, M.; Memiah, P. T. N.; Memish, Z. A.; Mendoza, W.; Mengistu, D. T.; Mensah, G. A.; Mensink, G. B. M.; Mereta, S. T.; Meretoja, A.; Meretoja, T. J.; Mestrovic, T.; Mezgebe, H. B.; Miazgowski, B.; Miazgowski, T.; Millear, A. I.; Miller, T. R.; Miller-Petrie, M. K.; Mini, G. K.; Mirarefin, M.; Mirica, A.; Mirrakhimov, E. M.; Misganaw, A. T.; Mitiku, H.; Moazen, B.; Mohajer, B.; Mohammad, K. A.; Mohammadi, M.; Mohammadifard, N.; Mohammadnia-Afrouzi, M.; Mohammed, S.; Mohebi, F.; Mokdad, A. H.; Molokhia, M.; Momeniha, F.; Monasta, L.; Moodley, Y.; Moradi, G.; Moradi-Lakeh, M.; Moradinazar, M.; Moraga, P.; Morawska, L.; Morgado-Da-Costa, J.; Morrison, S. D.; Moschos, M. M.; Mouodi, S.; Mousavi, S. M.; Mozaffarian, D.; Mruts, K. B.; Muche, A. A.; Muchie, K. F.; Mueller, U. O.; Muhammed, O. S.; Mukhopadhyay, S.; Muller, K.; Musa, K. I.; Mustafa, G.; Nabhan, A. F.; Naghavi, M.; Naheed, A.; Nahvijou, A.; Naik, G.; Naik, N.; Najafi, F.; Nangia, V.; Nansseu, J. R.; Nascimento, B. R.; Neal, B.; Neamati, N.; Negoi, I.; Negoi, R. I.; Neupane, S.; Newton, C. R. J.; Ngunjiri, J. W.; Nguyen, A. Q.; Nguyen, G.; Nguyen, H. T.; Nguyen, H. L. T.; Nguyen, H. T.; Nguyen, M.; Nguyen, N. B.; Nichols, E.; Nie, J.; Ningrum, D. N. A.; Nirayo, Y. L.; Nishi, N.; Nixon, M. R.; Nojomi,

https://doi.org/10.1021/acs.est.3c05404
Environ. Sci. Technol. 2024, 58, 3629−3640

M.; Nomura, S.; Norheim, O. F.; Noroozi, M.; Norrving, B.; Noubiap, J. J.; Nouri, H. R.; Nourollahpour Shiadeh, M.; Nowroozi, M. R.; Nsoesie, E. O.; Nyasulu, P. S.; Obermeyer, C. M.; Odell, C. M.; Ofori-Asenso, R.; Ogbo, F. A.; Oh, I.-H.; Oladimeji, O.; Olagunju, A. T.; Olagunju, T. O.; Olivares, P. R.; Olsen, H. E.; Olusanya, B. O.; Olusanya, J. O.; Ong, K. L.; Ong, S. K.; Oren, E.; Orpana, H. M.; Ortiz, A.; Ota, E.; Otstavnov, S. S.; Overland, S.; Owolabi, M. O.; M, P. A.; Pacella, R.; Pakhare, A. P.; Pakpour, A. H.; Pana, A.; Panda-Jonas, S.; Park, E.-K.; Parry, C. D. H.; Parsian, H.; Patel, S.; Pati, S.; Patil, S. T.; Patle, A.; Patton, G. C.; Paudel, D.; Paulson, K. R.; Paz Ballesteros, W. C.; Pearce, N.; Pereira, A.; Pereira, D. M.; Perico, N.; Pesudovs, K.; Petzold, M.; Pham, H. Q.; Phillips, M. R.; Pillay, J. D.; Piradov, M. A.; Pirsaheb, M.; Pischon, T.; Pishgar, F.; Plana-Ripoll, O.; Plass, D.; Polinder, S.; Polkinghorne, K. R.; Postma, M. J.; Poulton, R.; Pourshams, A.; Poustchi, H.; Prabhakaran, D.; Prakash, S.; Prasad, N.; Purcell, C. A.; Purwar, M. B.; Qorbani, M.; Radfar, A.; Rafay, A.; Rafiei, A.; Rahim, F.; Rahimi, Z.; Rahimi-Movaghar, A.; Rahimi-Movaghar, V.; Rahman, M.; Rahman, M. H. U.; Rahman, M. A.; Rai, R. K.; Rajati, F.; Rajsic, S.; Raju, S. B.; Ram, U.; Ranabhat, C. L.; Ranjan, P.; Rath, G. K.; Rawaf, D. L.; Rawaf, S.; Reddy, K. S.; Rehm, C. D.; Rehm, J.; Reiner, R. C.; Reitsma, M. B.; Remuzzi, G.; Renzaho, A. M. N.; Resnikoff, S.; Reynales-Shigematsu, L. M.; Rezaei, S.; Ribeiro, A. L. P.; Rivera, J. A.; Roba, K. T.; Rodríguez-Ramírez, S.; Roever, L.; Román, Y.; Ronfani, L.; Roshandel, G.; Rostami, A.; Roth, G. A.; Rothenbacher, D.; Roy, A.; Rubagotti, E.; Rushton, L.; Sabanayagam, C.; Sachdev, P. S.; Saddik, B.; Sadeghi, E.; Saeedi Moghaddam, S.; Safari, H.; Safari, Y.; Safari-Faramani, R.; Safdarian, M.; Safi, S.; Safiri, S.; Sagar, R.; Sahebkar, A.; Sahraian, M. A.; Sajadi, H. S.; Salam, N.; Salamati, P.; Saleem, Z.; Salimi, Y.; Salimzadeh, H.; Salomon, J. A.; Salvi, D. D.; Salz, I.; Samy, A. M.; Sanabria, J.; Sanchez-Niño, M. D.; Sánchez-Pimienta, T. G.; Sanders, T.; Sang, Y.; Santomauro, D. F.; Santos, I. S.; Santos, J. V.; Santric Milicevic, M. M.; Sao Jose, B. P.; Sardana, M.; Sarker, A. R.; Sarmiento-Suárez, R.; Sarrafzadegan, N.; Sartorius, B.; Sarvi, S.; Sathian, B.; Satpathy, M.; Sawant, A. R.; Sawhney, M.; Saylan, M.; Sayyah, M.; Schaeffner, E.; Schmidt, M. I.; Schneider, I. J. C.; Schöttker, B.; Schutte, A. E.; Schwebel, D. C.; Schwendicke, F.; Scott, J. G.; Seedat, S.; Sekerija, M.; Sepanlou, S. G.; Serre, M. L.; Serván-Mori, E.; Seyedmousavi, S.; Shabaninejad, H.; Shaddick, G.; Shafieesabet, A.; Shahbazi, M.; Shaheen, A. A.; Shaikh, M. A.; Shamah Levy, T.; Shams-Beyranvand, M.; Shamsi, M.; Sharafi, H.; Sharafi, K.; Sharif, M.; Sharif-Alhoseini, M.; Sharifi, H.; Sharma, J.; Sharma, M.; Sharma, R.; She, J.; Sheikh, A.; Shi, P.; Shibuya, K.; Shiferaw, M. S.; Shigematsu, M.; Shin, M.-J.; Shiri, R.; Shirkoohi, R.; Shiue, I.; Shokraneh, F.; Shoman, H.; Shrime, M. G.; Shupler, M. S.; Si, S.; Siabani, S.; Sibai, A. M.; Siddiqi, T. J.; Sigfusdottir, I. D.; Sigurvinsdottir, R.; Silva, D. A. S.; Silva, J. P.; Silveira, D. G. A.; Singh, J. A.; Singh, N. P.; Singh, V.; Sinha, D. N.; Skiadaresi, E.; Skirbekk, V.; Smith, D. L.; Smith, M.; Sobaih, B. H.; Sobhani, S.; Somayaji, R.; Soofi, M.; Sorensen, R. J. D.; Soriano, J. B.; Soyiri, I. N.; Spinelli, A.; Sposato, L. A.; Sreeramareddy, C. T.; Srinivasan, V.; Starodubov, V. I.; Steckling, N.; Stein, D. J.; Stein, M. B.; Stevanovic, G.; Stockfelt, L.; Stokes, M. A.; Sturua, L.; Subart, M. L.; Sudaryanto, A.; Sufiyan, M. A. B.; Sulo, G.; Sunguya, B. F.; Sur, P. J.; Sykes, B. L.; Szoeke, C. E. I.; Tabarés-Seisdedos, R.; Tabuchi, T.; Tadakamadla, S. K.; Takahashi, K.; Tandon, N.; Tassew, S. G.; Tavakkoli, M.; Taveira, N.; Tehrani-Banihashemi, A.; Tekalign, T. G.; Tekelemedhin, S. W.; Tekle, M. G.; Temesgen, H.; Temsah, M.-H.; Temsah, O.; Terkawi, A. S.; Tessema, B.; Teweldemedhin, M.; Thankappan, K. R.; Theis, A.; Thirunavukkarasu, S.; Thomas, H. J.; Thomas, M. L.; Thomas, N.; Thurston, G. D.; Tilahun, B.; Tillmann, T.; To, Q. G.; Tobollik, M.; Tonelli, M.; Topor-Madry, R.; Torre, A. E.; Tortajada-Girbés, M.; Touvier, M.; Tovani-Palone, M. R.; Towbin, J. A.; Tran, B. X.; Tran, K. B.; Truelsen, T. C.; Truong, N. T.; Tsadik, A. G.; Tudor Car, L.; Tuzcu, E. M.; Tymeson, H. D.; Tyrovolas, S.; Ukwaja, K. N.; Ullah, I.; Updike, R. L.; Usman, M. S.; Uthman, O. A.; Vaduganathan, M.; Vaezi, A.; Valdez, P. R.; Van Donkelaar, A.; Varavikova, E.; Varughese, S.; Vasankari, T. J.; Venkateswaran, V.; Venketasubramanian, N.; Villafaina, S.; Violante, F. S.; Vladimirov, S. K.; Vlassov, V.; Vollset, S. E.; Vos, T.; Vosoughi, K.; Vu, G. T.; Vujcic, I. S.; Wagnew, F. S.; Waheed, Y.; Waller, S. G.; Walson, J. L.; Wang, Y.; Wang, Y.; Wang, Y.-P.; Weiderpass, E.; Weintraub, R. G.; Weldegebreal, F.; Werdecker, A.; Werkneh, A. A.; West, J. J.; Westerman, R.; Whiteford, H. A.; Widecka, J.; Wijeratne, T.; Winkler, A. S.; Wiyeh, A. B.; Wiysonge, C. S.; Wolfe, C. D. A.; Wong, T. Y.; Wu, S.; Xavier, D.; Xu, G.; Yadgir, S.; Yadollahpour, A.; Yahyazadeh Jabbari, S. H.; Yamada, T.; Yan, L. L.; Yano, Y.; Yaseri, M.; Yasin, Y. J.; Yeshaneh, A.; Yimer, E. M.; Yip, P.; Yisma, E.; Yonemoto, N.; Yoon, S.-J.; Yotebieng, M.; Younis, M. Z.; Yousefifard, M.; Yu, C.; Zaidi, Z.; Zaman, S. B.; Zamani, M.; Zavala-Arciniega, L.; Zhang, A. L.; Zhang, H.; Zhang, K.; Zhou, M.; Zimsen, S. R. M.; Zodpey, S.; Murray, C. J. L. Global, regional, and national comparative risk assessment of 84 behavioural, environmental and occupational, and metabolic risks or clusters of risks for 195 countries and territories, 1990−2017: a systematic analysis for the Global Burden of Disease Study 2017. *Lancet* **2018**, *392* (10159), 1923−1994.

(2) Lelieveld, J.; Evans, J. S.; Fnais, M.; Giannadaki, D.; Pozzer, A. The contribution of outdoor air pollution sources to premature mortality on a global scale. *Nature* **2015**, *525* (7569), 367−371.

(3) Zhang, Q.; Zheng, Y.; Tong, D.; Shao, M.; Wang, S.; Zhang, Y.; Xu, X.; Wang, J.; He, H.; Liu, W.; Ding, Y.; Lei, Y.; Li, J.; Wang, Z.; Zhang, X.; Wang, Y.; Cheng, J.; Liu, Y.; Shi, Q.; Yan, L.; Geng, G.; Hong, C.; Li, M.; Liu, F.; Zheng, B.; Cao, J.; Ding, A.; Gao, J.; Fu, Q.; Huo, J.; Liu, B.; Liu, Z.; Yang, F.; He, K.; Hao, J. Drivers of improved $PM_{2.5}$ air quality in China from 2013 to 2017. *Proc. Natl. Acad. Sci. U. S. A.* **2019**, *116* (49), 24463−24469.

(4) Wang, Y.; Gao, W.; Wang, S.; Song, T.; Gong, Z.; Ji, D.; Wang, L.; Liu, Z.; Tang, G.; Huo, Y.; Tian, S.; Li, J.; Li, M.; Yang, Y.; Chu, B.; Petäjä, T.; Kerminen, V.-M.; He, H.; Hao, J.; Kulmala, M.; Wang, Y.; Zhang, Y. Contrasting trends of $PM_{2.5}$ and surface-ozone concentrations in China from 2013 to 2017. *National Science Review* **2020**, *7* (8), 1331−1339.

(5) Colmer, J.; Hardman, I.; Shimshack, J.; Voorheis, J. Disparities in $PM_{2.5}$ air pollution in the United States. *Science* **2020**, *369* (6503), 575−578.

(6) Meng, X.; Hand, J. L.; Schichtel, B. A.; Liu, Y. Space-time trends of $PM_{2.5}$ constituents in the conterminous United States estimated by a machine learning approach, 2005−2015. *Environ. Int.* **2018**, *121*, 1137−1147.

(7) Hammer, M. S.; van Donkelaar, A.; Li, C.; Lyapustin, A.; Sayer, A. M.; Hsu, N. C.; Levy, R. C.; Garay, M. J.; Kalashnikova, O. V.; Kahn, R. A.; Brauer, M.; Apte, J. S.; Henze, D. K.; Zhang, L.; Zhang, Q.; Ford, B.; Pierce, J. R.; Martin, R. V. Global Estimates and Long-Term Trends of Fine Particulate Matter Concentrations (1998−2018). *Environ. Sci. Technol.* **2020**, *54* (13), 7879−7890.

(8) Tsyro, S.; Aas, W.; Colette, A.; Andersson, C.; Bessagnet, B.; Ciarelli, G.; Couvidat, F.; Cuvelier, K.; Manders, A.; Mar, K.; Mircea, M.; Otero, N.; Pay, M. T.; Raffort, V.; Roustan, Y.; Theobald, M. R.; Vivanco, M. G.; Fagerli, H.; Wind, P.; Briganti, G.; Cappelletti, A.; D'Isidoro, M.; Adani, M. Eurodelta multi-model simulated and observed PM trends in Europe in the period of 1990−2010. *Atmos. Chem. Phys.* **2021**, *22*, 7207−7257.

(9) Southerland, V. A.; Brauer, M.; Mohegh, A.; Hammer, M. S.; van Donkelaar, A.; Martin, R. V.; Apte, J. S.; Anenberg, S. C. Global urban temporal trends in fine particulate matter ($PM_{2.5}$) and attributabe health burdens: estimates from global datasets. *The Lancet Planetary. Health* **2022**, *6* (2), e139−e146.

(10) McDuffie, E. E.; Martin, R. V.; Spadaro, J. V.; Burnett, R.; Smith, S. J.; O'Rourke, P.; Hammer, M. S.; van Donkelaar, A.; Bindle, L.; Shah, V.; Jaeglé, L.; Luo, G.; Yu, F.; Adeniran, J. A.; Lin, J.; Brauer, M. Source sector and fuel contributions to ambient $PM_{2.5}$ and attributable mortality across multiple spatial scales. *Nat. Commun.* **2021**, *12* (1), 3594.

(11) Daellenbach, K. R.; Uzu, G.; Jiang, J.; Cassagnes, L.-E.; Leni, Z.; Vlachou, A.; Stefenelli, G.; Canonaco, F.; Weber, S.; Segers, A.; Kuenen, J. J. P.; Schaap, M.; Favez, O.; Albinet, A.; Aksoyoglu, S.; Dommen, J.; Baltensperger, U.; Geiser, M.; El Haddad, I.; Jaffrezo, J.-L.; Prévôt, A. S. H. Sources of particulate-matter air pollution and its oxidative potential in Europe. *Nature* **2020**, *587* (7834), 414−419.

https://doi.org/10.1021/acs.est.3c05404
Environ. Sci. Technol. 2024, 58, 3629−3640

(12) Wu, D.; Zheng, H.; Li, Q.; Jin, L.; Lyu, R.; Ding, X.; Huo, Y.; Zhao, B.; Jiang, J.; Chen, J.; Li, X.; Wang, S. Toxic potency-adjusted control of air pollution for solid fuel combustion. *Nature Energy* **2022**, *7* (2), 194−202.
(13) Jin, L.; Luo, X.; Fu, P.; Li, X. Airborne particulate matter pollution in urban China: a chemical mixture perspective from sources to impacts. *National Science Review* **2017**, *4* (4), 593−610.
(14) Jin, L.; Xie, J.; Wong, C. K. C.; Chan, S. K. Y.; Abbaszade, G.; Schnelle-Kreis, J.; Zimmermann, R.; Li, J.; Zhang, G.; Fu, P.; Li, X. Contributions of City-Specific Fine Particulate Matter ($PM_{2.5}$) to Differential In Vitro Oxidative Stress and Toxicity Implications between Beijing and Guangzhou of China. *Environ. Sci. Technol.* **2019**, *53* (5), 2881−2891.
(15) Park, M.; Joo, H. S.; Lee, K.; Jang, M.; Kim, S. D.; Kim, I.; Borlaza, L. J. S.; Lim, H.; Shin, H.; Chung, K. H.; Choi, Y.-H.; Park, S. G.; Bae, M.-S.; Lee, J.; Song, H.; Park, K. Differential toxicities of fine particulate matters from various sources. *Sci. Rep.* **2018**, *8* (1), No. 17007.
(16) Antoniadis, V.; Shaheen, S. M.; Levizou, E.; Shahid, M.; Niazi, N. K.; Vithanage, M.; Ok, Y. S.; Bolan, N.; Rinklebe, J. A critical prospective analysis of the potential toxicity of trace element regulation limits in soils worldwide: Are they protective concerning health risk assessment? - A review. *Environ. Int.* **2019**, *127*, 819−847.
(17) Li, X.; Jin, L.; Kan, H. Air pollution: a global problem needs local fixes. *Nature* **2019**, *570* (7762), 437−439.
(18) Ali, M. U.; Liu, G.; Yousaf, B.; Ullah, H.; Abbas, Q.; Munir, M. A. M. A systematic review on global pollution status of particulate matter-associated potential toxic elements and health perspectives in urban environment. *Environmental geochemistry and health* **2019**, *41* (3), 1131−1162.
(19) Zhuang, G.; Yi, Z.; Duce, R. A.; Brown, P. R. Link between iron and sulphur cycles suggested by detection of Fe(n) in remote marine aerosols. *Nature* **1992**, *355* (6360), 537−539.
(20) Colombo, M.; Li, J.; Rogalla, B.; Allen, S. E.; Maldonado, M. T. Particulate trace element distributions along the Canadian Arctic GEOTRACES section: shelf-water interactions, advective transport and contrasting biological production. *Geochim Cosmochim Ac* **2022**, *323*, 183−201.
(21) Cheng, K.; Chang, Y.; Kuang, Y.; Khan, R.; Zou, Z. Elucidating the responses of highly time-resolved $PM_{2.5}$ related elements to extreme emission reductions. *Environ. Res.* **2022**, *206*, No. 112624.
(22) Li, W.; Dryfhout-Clark, H.; Hung, H. PM_{10}-bound trace elements in the Great Lakes Basin (1988−2017) indicates effectiveness of regulatory actions, variations in sources and reduction in human health risks. *Environ. Int.* **2020**, *143*, No. 106008.
(23) Cheng, K.; Chang, Y.; Kuang, Y.; Ling, Q.; Zou, Z.; Huang, R.-J. Multiple-Year Changes (2014−2018) in Particulate Vanadium Linked to Shipping Regulations in the World's Largest Port Region. *ACS Earth and Space Chemistry* **2022**, *6* (2), 415−420.
(24) Yan, R.-H.; Peng, X.; Lin, W.; He, L.-Y.; Wei, F.-H.; Tang, M.-X.; Huang, X.-F. Trends and Challenges Regarding the Source-Specific Health Risk of PM2.5-Bound Metals in a Chinese Megacity from 2014 to 2020. *Environ. Sci. Technol.* **2022**, *56*, 6996−7005, DOI: 10.1021/acs.est.1c06948.
(25) Huang, R.-J.; Cheng, R.; Jing, M.; Yang, L.; Li, Y.; Chen, Q.; Chen, Y.; Yan, J.; Lin, C.; Wu, Y.; Zhang, R.; El Haddad, I.; Prevot, A. S. H.; O'Dowd, C. D.; Cao, J. Source-Specific Health Risk Analysis on Particulate Trace Elements: Coal Combustion and Traffic Emission As Major Contributors in Wintertime Beijing. *Environ. Sci. Technol.* **2018**, *52* (19), 10967−10974.
(26) Liu, X.; Ouyang, W.; Shu, Y.; Tian, Y.; Feng, Y.; Zhang, T.; Chen, W. Incorporating bioaccessibility into health risk assessment of heavy metals in particulate matter originated from different sources of atmospheric pollution. *Environ. Pollut.* **2019**, *254*, No. 113113.
(27) Huang, R. J.; Zhang, Y.; Bozzetti, C.; Ho, K. F.; Cao, J. J.; Han, Y.; Daellenbach, K. R.; Slowik, J. G.; Platt, S. M.; Canonaco, F.; Zotter, P.; Wolf, R.; Pieber, S. M.; Bruns, E. A.; Crippa, M.; Ciarelli, G.; Piazzalunga, A.; Schwikowski, M.; Abbaszade, G.; Schnelle-Kreis, J.; Zimmermann, R.; An, Z.; Szidat, S.; Baltensperger, U.; El Haddad, I.; Prévôt, A. S. High secondary aerosol contribution to particulate pollution during haze events in China. *Nature* **2014**, *514* (7521), 218−222.
(28) Xie, J.; Jin, L.; Cui, J.; Luo, X.; Li, J.; Zhang, G.; Li, X. Health risk-oriented source apportionment of $PM_{2.5}$-associated trace metals. *Environ. Pollut.* **2020**, *262*, No. 114655.
(29) Chang, Y.; Huang, K.; Xie, M.; Deng, C.; Zou, Z.; Liu, S.; Zhang, Y. First long-term and near real-time measurement of trace elements in China's urban atmosphere: temporal variability, source apportionment and precipitation effect. *Atmos. Chem. Phys.* **2018**, *18* (16), 11793−11812.
(30) Furger, M.; Minguillón, M. C.; Yadav, V.; Slowik, J. G.; Hüglin, C.; Fröhlich, R.; Petterson, K.; Baltensperger, U.; Prévôt, A. S. H. Elemental composition of ambient aerosols measured with high temporal resolution using an online XRF spectrometer. *Atmos. Meas. Technol.* **2017**, *10* (6), 2061−2076.
(31) Lee, J.; Ryu, J.-S.; Jeong, S.; Kim, J.; Jeong, H.; Ra, K.; Yang, M.; Chang, H. J. Elemental and isotopic compositions in blank filters collecting atmospheric particulates. *J. Anal. Sci. Technol.* **2021**, *12* (1), 27.
(32) Resongles, E.; Dietze, V.; Green David, C.; Harrison Roy, M.; Ochoa-Gonzalez, R.; Tremper Anja, H.; Weiss, D. J. Strong evidence for the continued contribution of lead deposited during the 20th century to the atmospheric environment in London of today. *Proc. Natl. Acad. Sci. U. S. A.* **2021**, *118* (26), No. e2102791118.
(33) Li, Q.; Liu, H.; Alattar, M.; Jiang, S.; Han, J.; Ma, Y.; Jiang, C. The preferential accumulation of heavy metals in different tissues following frequent respiratory exposure to $PM_{2.5}$ in rats. *Sci. Rep.* **2015**, *5*, No. 16936.
(34) IRIS. *IRIS Assessments*. https://www.epa.gov/iris (accessed March 2022).
(35) IARC. *IARC Monographs on the Evaluation of Carcinogenic Risks to Humans*. https://monographs.iarc.who.int/list-ofclassifications (accessed March 2022).
(36) Duan, X. *Highlights of the Chinese exposure factors handbook*; Academic Press, 2015.
(37) Shen, G.; Ru, M.; Du, W.; Zhu, X.; Zhong, Q.; Chen, Y.; Shen, H.; Yun, X.; Meng, W.; Liu, J.; Cheng, H.; Hu, J.; Guan, D.; Tao, S. Impacts of air pollutants from rural Chinese households under the rapid residential energy transition. *Nat. Commun.* **2019**, *10* (1), 3405.
(38) Peng, L.; Zhang, Q.; Yao, Z.; Mauzerall, D. L.; Kang, S.; Du, Z.; Zheng, Y.; Xue, T.; He, K. Underreported coal in statistics: A survey-based solid fuel consumption and emission inventory for the rural residential sector in China. *Applied Energy* **2019**, *235*, 1169−1182.
(39) Yun, X.; Shen, G.; Shen, H.; Meng, W.; Chen, Y.; Xu, H.; Ren, Y.; Zhong, Q.; Du, W.; Ma, J.; Cheng, H.; Wang, X.; Liu, J.; Wang, X.; Li, B.; Hu, J.; Wan, Y.; Tao, S. Residential solid fuel emissions contribute significantly to air pollution and associated health impacts in China. *Sci. Adv.* **2020**, *6* (44), No. eaba7621.
(40) Lin, C.; Huang, R.-J.; Ceburnis, D.; Buckley, P.; Preissler, J.; Wenger, J.; Rinaldi, M.; Facchini, M. C.; O'Dowd, C.; Ovadnevaite, J. Extreme air pollution from residential solid fuel burning. *Nature Sustainability* **2018**, *1* (9), 512−517.
(41) Echalar, F.; Gaudichet, A.; Cachier, H.; Artaxo, P. Aerosol emissions by tropical forest and savanna biomass burning: Characteristic trace elements and fluxes. *Geophys. Res. Lett.* **1995**, *22* (22), 3039−3042.
(42) Andreae, M. O.; Merlet, P. Emission of trace gases and aerosols from biomass burning. *Global Biogeochem. Cy.* **2001**, *15* (4), 955−966.
(43) Tang, L.; Qu, J.; Mi, Z.; Bo, X.; Chang, X.; Anadon, L. D.; Wang, S.; Xue, X.; Li, S.; Wang, X.; Zhao, X. Substantial emission reductions from Chinese power plants after the introduction of ultra-low emissions standards. *Nature Energy* **2019**, *4* (11), 929−938.
(44) Zheng, B.; Tong, D.; Li, M.; Liu, F.; Hong, C.; Geng, G.; Li, H.; Li, X.; Peng, L.; Qi, J.; Yan, L.; Zhang, Y.; Zhao, H.; Zheng, Y.; He, K.; Zhang, Q. Trends in China's anthropogenic emissions since 2010 as the consequence of clean air actions. *Atmos. Chem. Phys.* **2018**, *18* (19), 14095−14111.

(45) Xiao, Q.; Geng, G.; Xue, T.; Liu, S.; Cai, C.; He, K.; Zhang, Q. Tracking $PM_{2.5}$ and O_3 Pollution and the Related Health Burden in China 2013−2020. *Environ. Sci. Technol.* **2022**, *56*, 6922−6932, DOI: 10.1021/acs.est.1c04548.

https://doi.org/10.1021/acs.est.3c05404
Environ. Sci. Technol. 2024, 58, 3629−3640